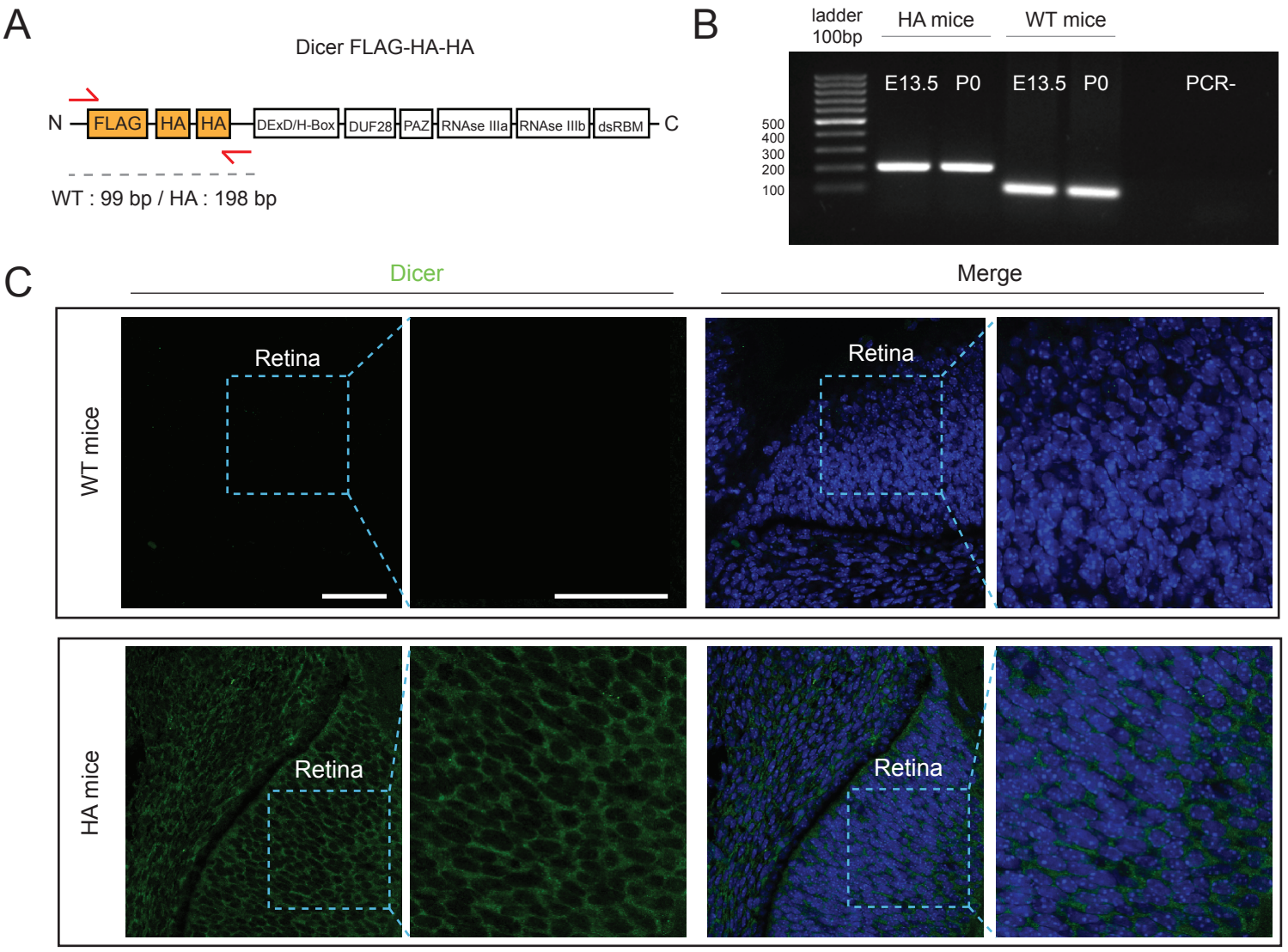

D

dre-let-7b	dre-mir-10b-2	dre-mir-124-2	dre-mir-124-5	dre-mir-128-1	dre-mir-139	dre-mir-25	dre-mir-26a-1	dre-mir-454b	dre-mir-455-1
dre-mir-726	xla-mir-1306	xla-mir-133a	xla-mir-133b	xla-mir-133d	xla-mir-142	xla-mir-15c	xla-mir-18	xla-mir-194	xla-mir-19b
xla-mir-1b	xla-mir-20	xla-mir-205	xla-mir-223	xla-mir-23a	xla-mir-24b	xla-mir-363	xla-mir-427	xla-mir-428	xla-mir-703
xla-mir-92a-1	xla-mir-92a-2	xtr-let-7a	xtr-let-7b	xtr-let-7c	xtr-let-7e-1	xtr-let-7e-2	xtr-let-7f	xtr-let-7g	xtr-let-7i
xtr-mir-100	xtr-mir-101a-1	xtr-mir-101a-2	xtr-mir-103-1	xtr-mir-103-2	xtr-mir-106	xtr-mir-107	xtr-mir-10a	xtr-mir-10c	xtr-mir-122
xtr-mir-124	xtr-mir-125a	xtr-mir-125b-1	xtr-mir-125b-2	xtr-mir-126	xtr-mir-128-2	xtr-mir-129-1	xtr-mir-129-2	xtr-mir-130a	xtr-mir-130b
xtr-mir-130c	xtr-mir-132	xtr-mir-133a	xtr-mir-133c	xtr-mir-135-1	xtr-mir-135-2	xtr-mir-137	xtr-mir-138	xtr-mir-139	xtr-mir-140
xtr-mir-143	xtr-mir-144	xtr-mir-145	xtr-mir-146a	xtr-mir-146b	xtr-mir-148a	xtr-mir-148b	xtr-mir-150	xtr-mir-153-1	xtr-mir-153-2
xtr-mir-155	xtr-mir-15a	xtr-mir-15b	xtr-mir-16a	xtr-mir-16b	xtr-mir-16c	xtr-mir-17	xtr-mir-181a-1	xtr-mir-181a-2	xtr-mir-181b-1
xtr-mir-181b-2	xtr-mir-182	xtr-mir-183	xtr-mir-184	xtr-mir-18a	xtr-mir-190	xtr-mir-191	xtr-mir-192	xtr-mir-193	xtr-mir-194-1
xtr-mir-194-2	xtr-mir-196a	xtr-mir-196b	xtr-mir-199a	xtr-mir-199b	xtr-mir-19a	xtr-mir-19b-2	xtr-mir-1a-1	xtr-mir-1a-2	xtr-mir-200a
xtr-mir-200b	xtr-mir-203	xtr-mir-204-1	xtr-mir-204-2	xtr-mir-205a	xtr-mir-205b	xtr-mir-206	xtr-mir-208	xtr-mir-20a	xtr-mir-210
xtr-mir-212	xtr-mir-214	xtr-mir-215	xtr-mir-216	xtr-mir-217	xtr-mir-218-1	xtr-mir-218-2	xtr-mir-2184	xtr-mir-2188	xtr-mir-219
xtr-mir-22	xtr-mir-221	xtr-mir-222	xtr-mir-23a-2	xtr-mir-23b	xtr-mir-24a	xtr-mir-24b	xtr-mir-26-2	xtr-mir-27a	xtr-mir-27b
xtr-mir-27c-1	xtr-mir-29a	xtr-mir-29c	xtr-mir-29d	xtr-mir-301-1	xtr-mir-301-2	xtr-mir-302	xtr-mir-30a	xtr-mir-30b	xtr-mir-30c-1
xtr-mir-30c-2	xtr-mir-30d	xtr-mir-30e	xtr-mir-338-1	xtr-mir-338-2	xtr-mir-33a	xtr-mir-33b	xtr-mir-34a	xtr-mir-34b-3	xtr-mir-363
xtr-mir-365-1	xtr-mir-375	xtr-mir-383	xtr-mir-425	xtr-mir-427-1	xtr-mir-428b	xtr-mir-429	xtr-mir-449a	xtr-mir-449b	xtr-mir-449c
xtr-mir-451 *	xtr-mir-489	xtr-mir-499	xtr-mir-7-1	xtr-mir-7-2	xtr-mir-7-3	xtr-mir-92b	xtr-mir-9-3	xtr-mir-9406	xtr-mir-96
xtr-mir-98	xtr-mir-99	xtr-mir-9a-1	xtr-mir-9a-2	xtr-mir-9b					

More than 5 reads spanning the whole loop
Less than 5 reads spanning the whole loop
No reads spanning the loop region
* Dicer independent miRNA biogenesis

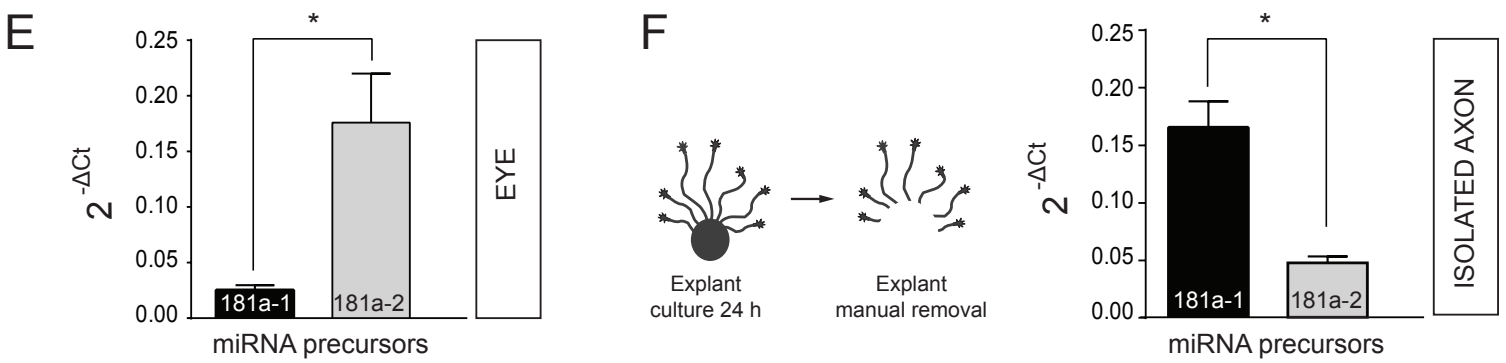

Supplementary Figure 1

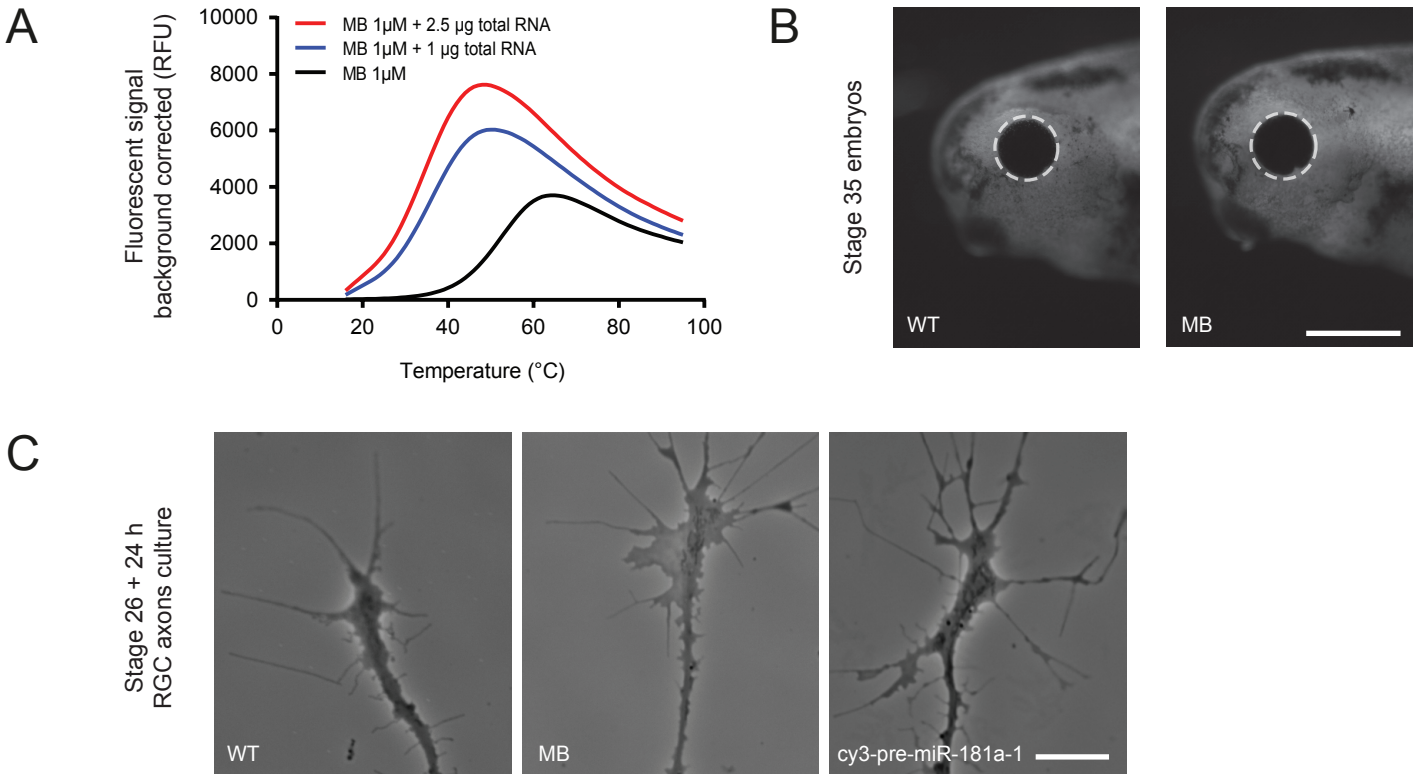

Supplementary Figure 2

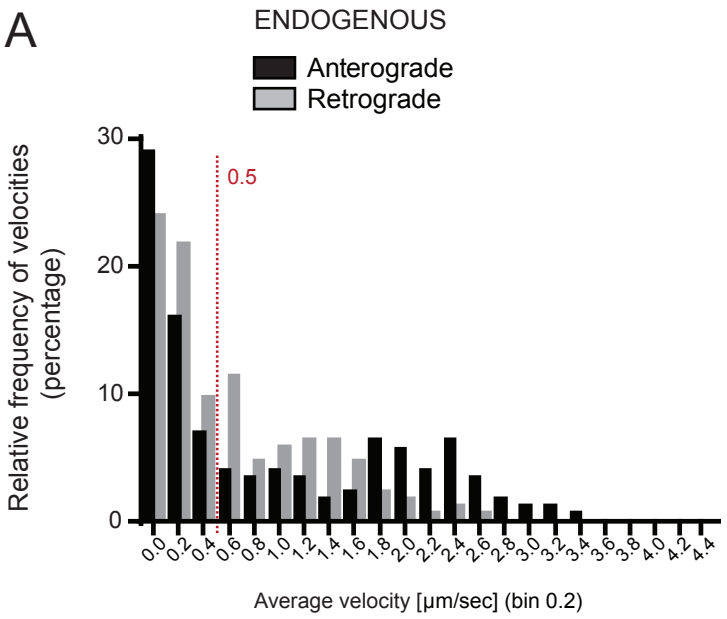

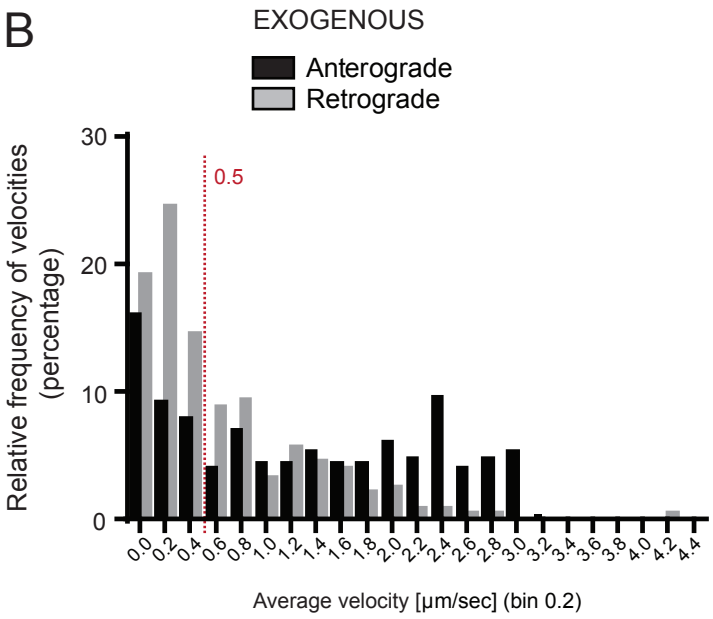

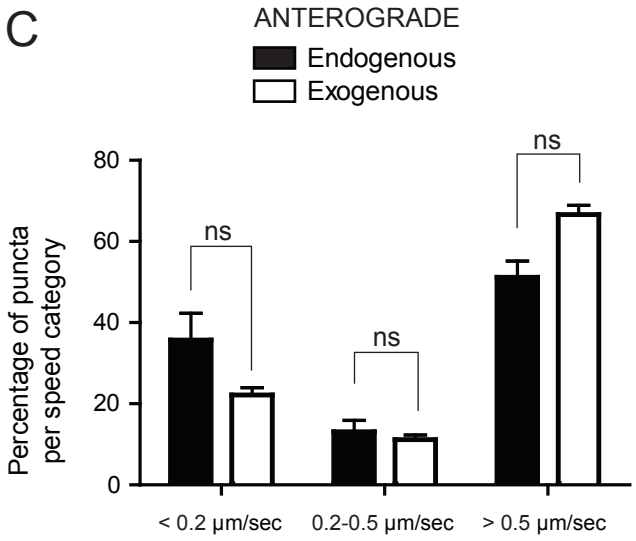

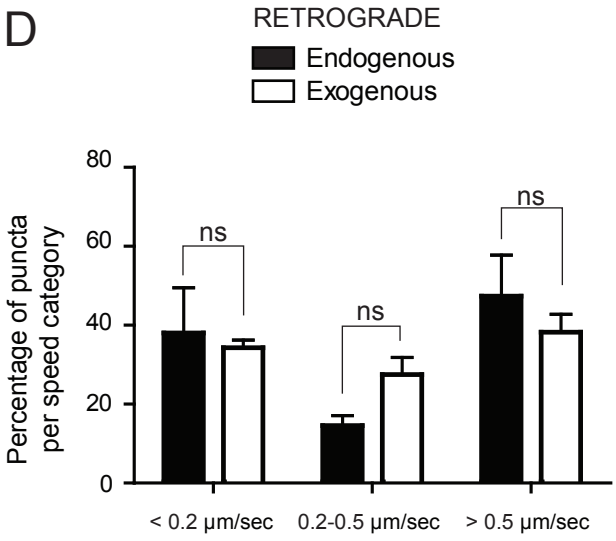

Supplementary Figure 3

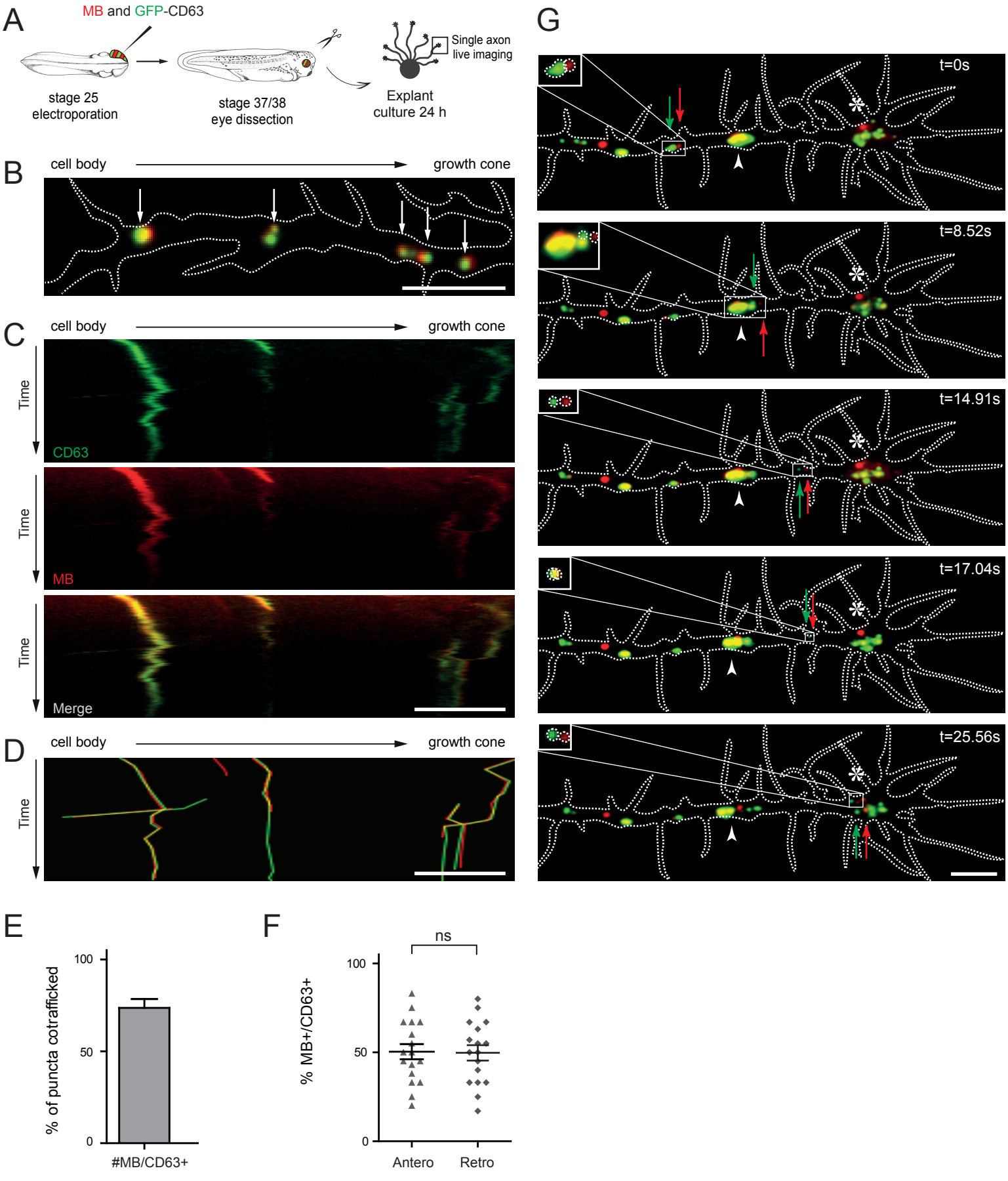

Supplementary Figure 4

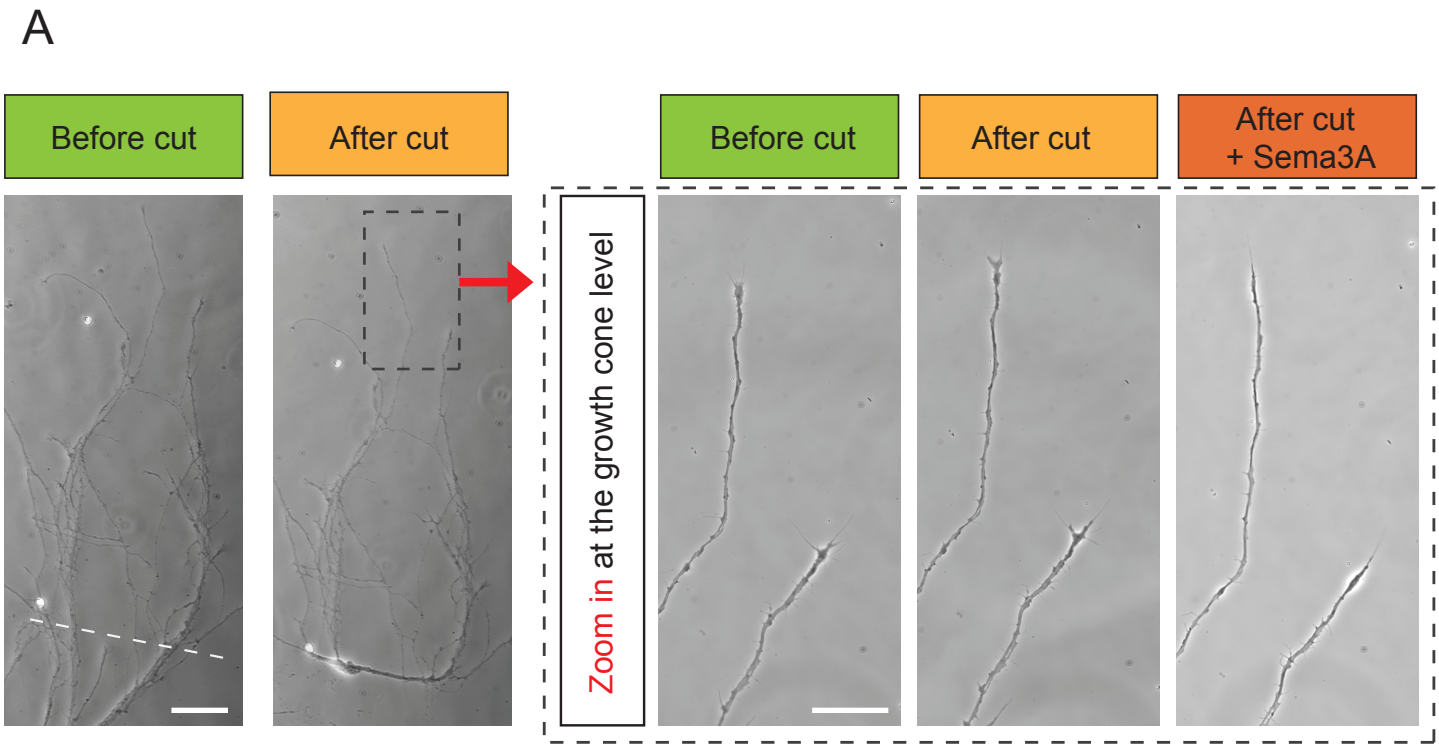

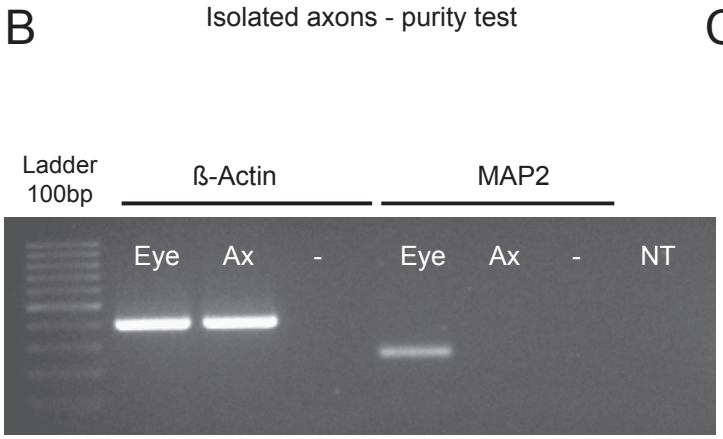

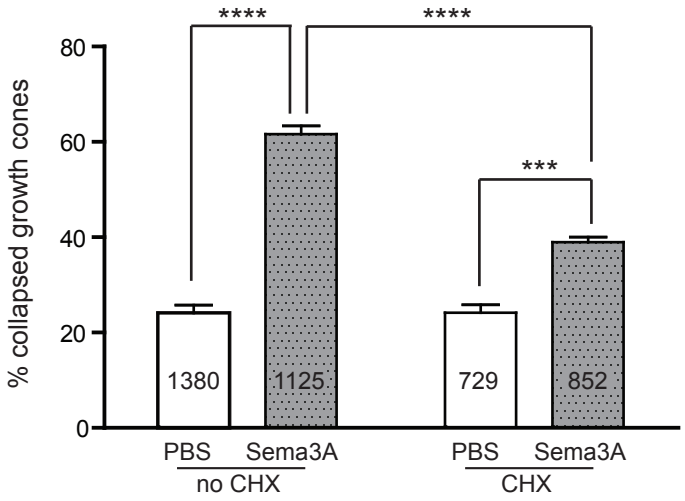

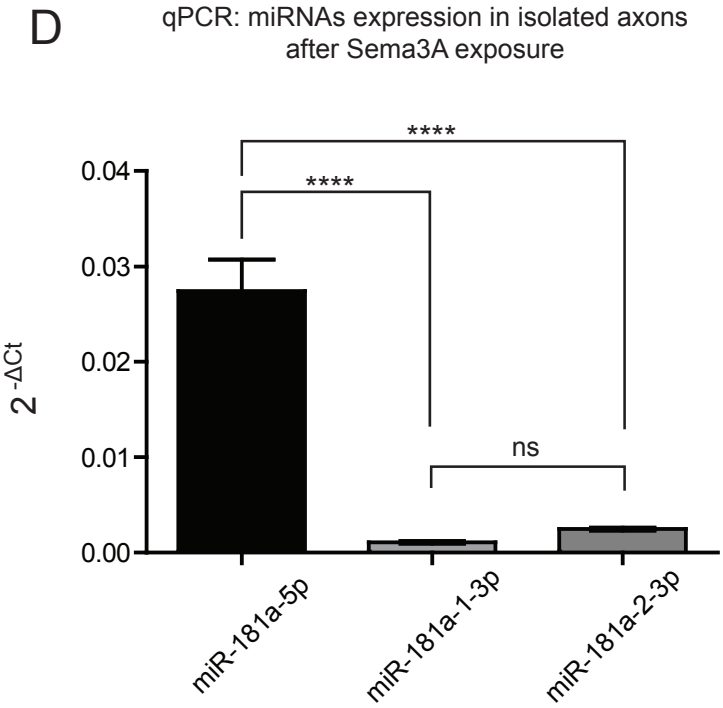

Supplementary Figure 5

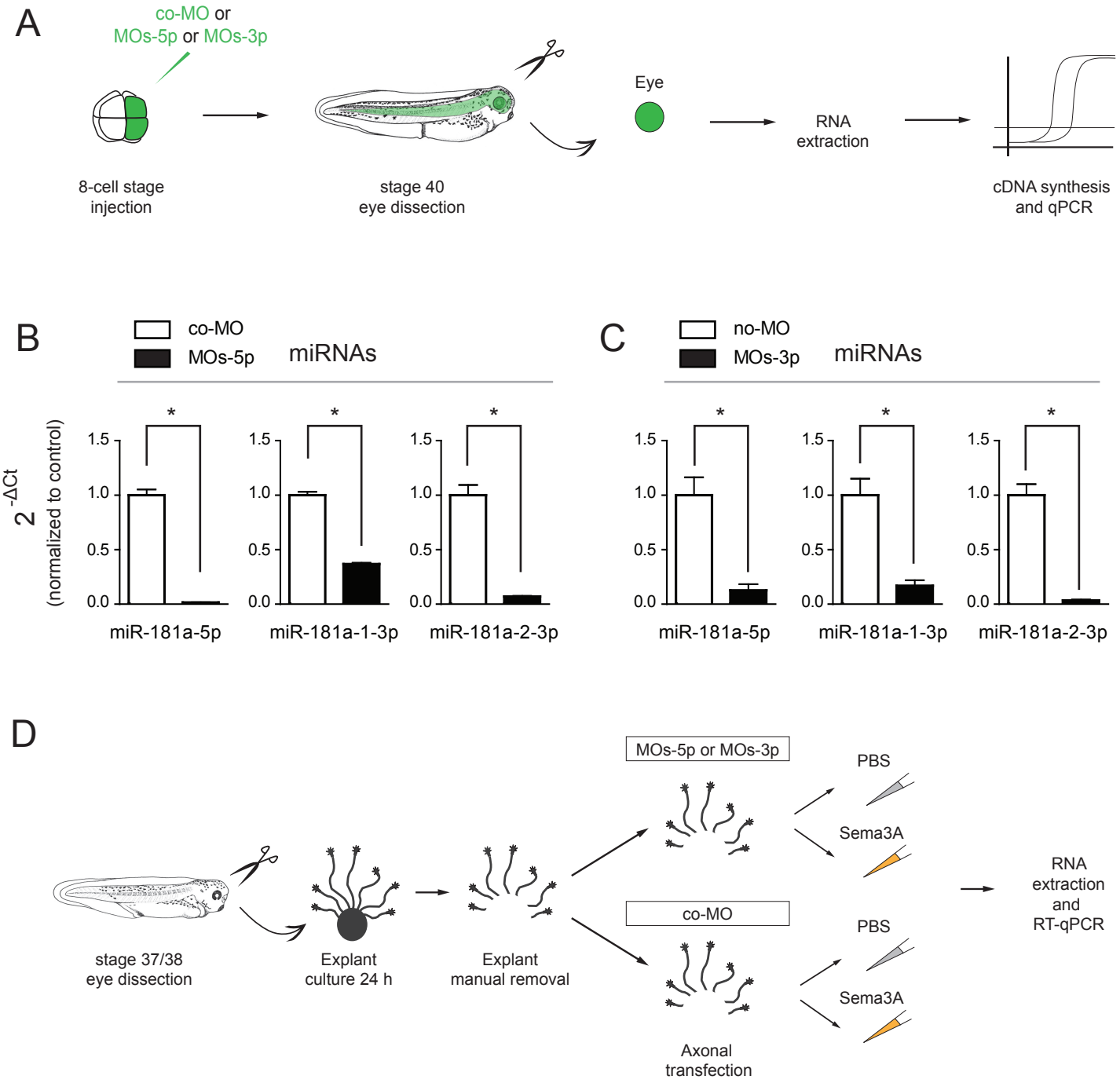

Supplementary Figure 6

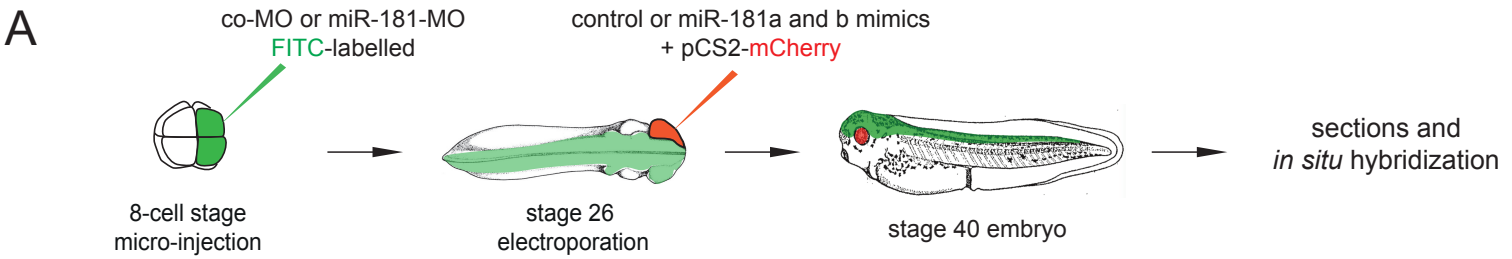

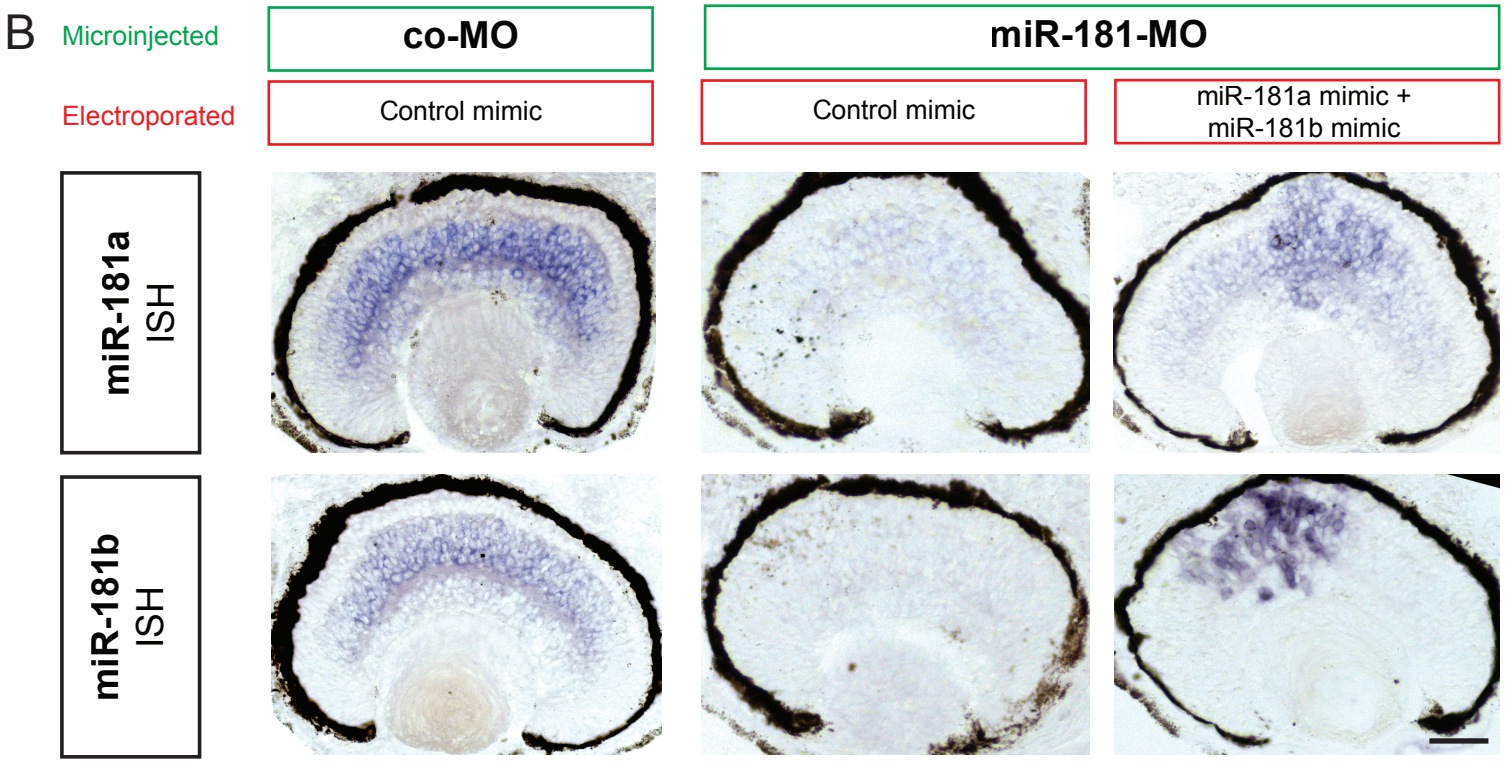

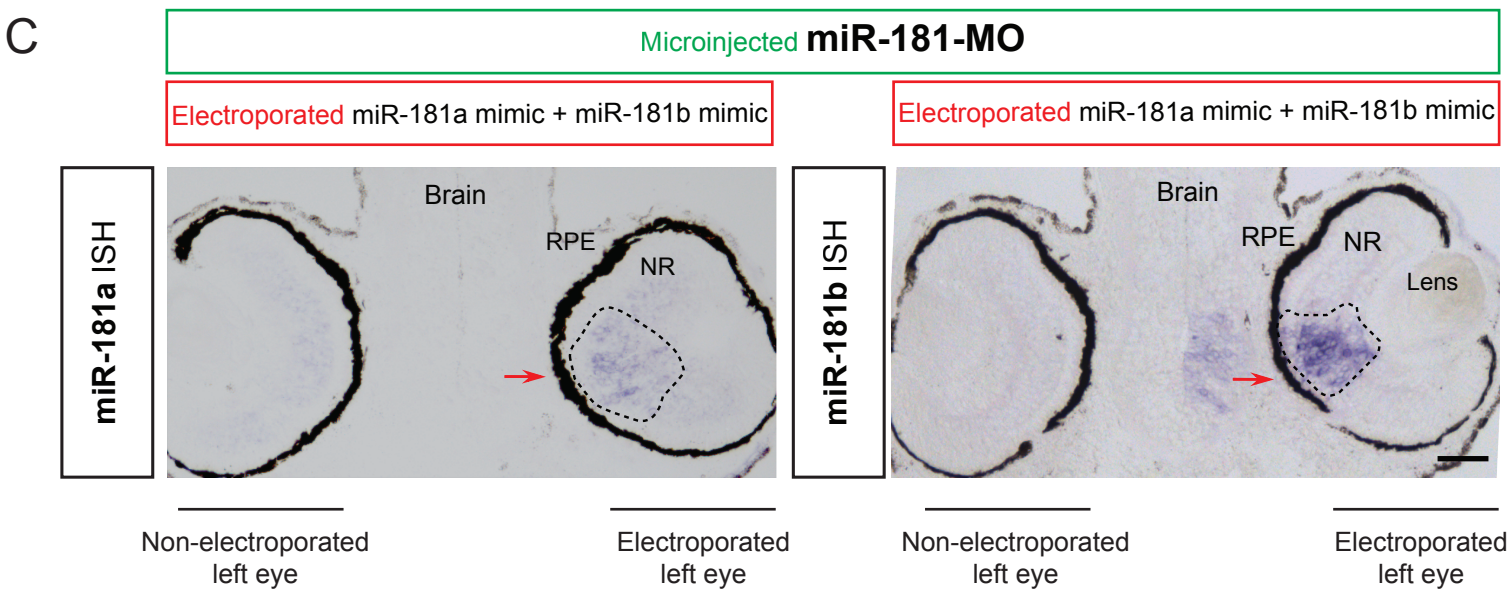

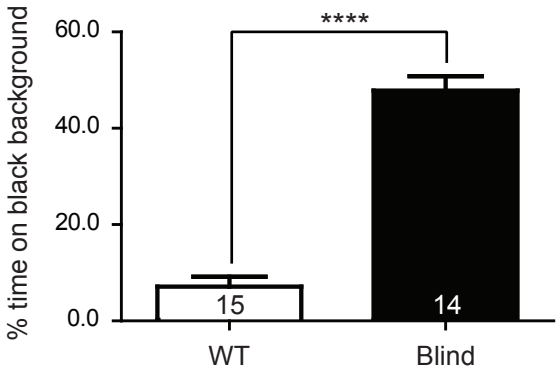

Supplementary Figure 7

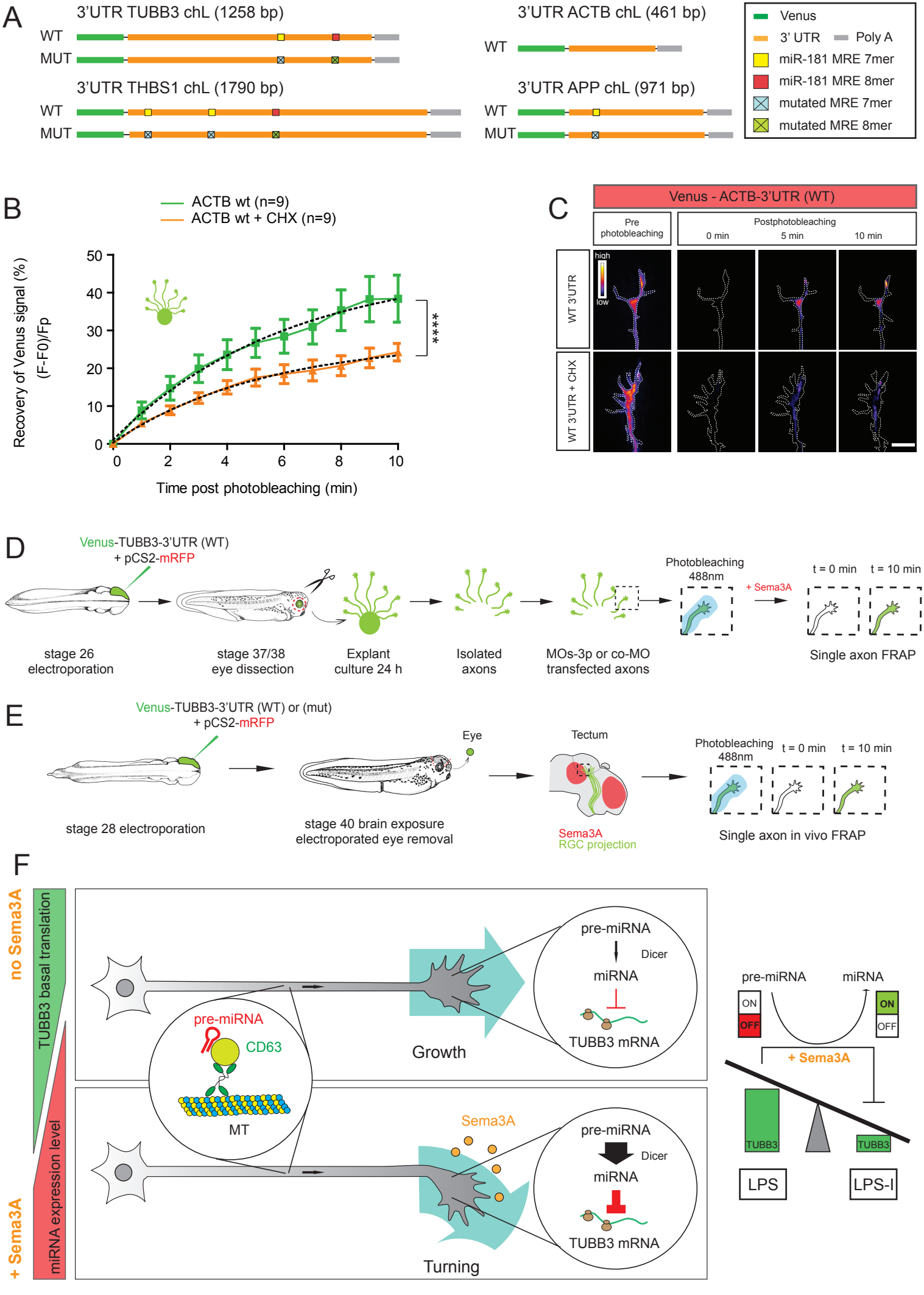

Supplementary Figure 8

[S1] Figure S1: Dicer and pre-miRNAs are present in RGCs axonal compartment, related to Figure 1
(A) Schematic of Dicer-FLAG-HA_2. Red arrows indicate primers used for the genotyping spanning the FLAG-HA_2 region. **(B)** Genotyping PCR. **(C)** Representative retina stained for anti-HA antibody. **(D)** List of axonal miRNAs derived from Bellon et al. 2017. Pre-miRNAs with more than 5 reads mapping the hairpin loop were considered abundant. **(E, F)** Quantification of the expression levels of miR-181a-1- and miR-181a-2-precursors with the $2^{\wedge(-\Delta Ct)}$ method, using U6 as normalizer, in eye **(E)** or isolated axons **(F)**.
Values are mean ± SEM (E, F). Statistics: * $p<0.05$. Data were not normally distributed (Shapiro-Wilk test), two-tailed Mann Whitney test, n=4 independent experiments (RNA was collected from 20 eyes or from isolated axons derived from 40 explants for each experiment). Abbreviations: WT, wild type; HA, Dicer-FLAG-HA_2; bp, base pair; E13.5, embryonic day 13.5; P0, post-natal day 0; PCR -, no template PCR negative control. Scale bars: 50 µm (C).

[S2] Figure S2: Pre-miR-181a-1 is trafficked in RGC axons, related to Figure 2
(A) Thermal denaturation of 1 µM MB in the absence or presence of total cellular RNA (2.5 or 1 µg) extracted from stage 40 eyes. Each melting curve represents the average of three separate experiments. **(B)** *Xenopus* head from WT or MB (20 µM) electroporated embryos. The eye is delineated with dashed lines. **(C)** Phase images of RGC axonal growth cones derived from WT, MB (20 µM) or cy3-pre-miR-181a-1 (10 µM) electroporated embryos. Note similar eye size and the stereotypical growth cone shape regardless of treatment indicating lack of MB toxicity. Abbreviations: MB, molecular beacon; WT, wild type. Scale bars: 500 µm (B), 10 µm (C).

[S3] Figure S3: Pre-miR-181a-1 is actively trafficked in RGC axons, related to Figure 3
(A, B) Relative frequency distribution (in percentage) of puncta velocities. Each bin corresponds to 0.2 µm/s. The dotted line indicates 0.5 µm/s. **(C, D)** Frequency distribution (in percentage) of puncta per speed category. (A-D) Endogenous and exogenous correspond to MB and cy3-pre-miR-181a-1 puncta, respectively.
Values are mean ± SEM (C, D). Statistics: **(C, D)** Two-way ANOVA followed by Tukey's multiple comparison post-hoc test. Endogenous, n=3; exogenous, n=4 independent experiments. Total number of analyzed puncta: 117 (endogenous anterograde), 176 (endogenous retrograde), 233 (exogenous anterograde), 251 (exogenous retrograde). Abbreviations: ns, not significant.

[S4] Figure S4: Pre-miR-181a-1 trafficking is vesicle mediated, related to Figure 4
(A) Schematic of the experimental paradigm. 5 µM MB and 0.5 µg/ul pCS2-CD63-eGFP were co-electroporated. **(B)** Snapshot of representative axon where MB-labeled pre-miR-181a-1 (red) and CD63-GFP-labeled vesicles (green) are co-trafficked (white arrows). **(C)** Representative kymographs generated from acquired time-lapse. **(D)** Composite kymograph shown in (C) where the individual traces where drawn and color coded. Yellow trajectories represent MB-labeled pre-miRNA (red) and CD63-GFP-labeled vesicle (green) co-trafficked. **(E)** Frequency and **(F)** frequency distribution (in percentage) of MB-labeled pre-miR-181a-1 co-trafficked with CD63-GFP-positive vesicles. Each dot corresponds to % of MB+/CD63+ co-trafficked puncta within each axon (F). **(G)** Representative time-lapse depicting MB-labeled pre-miR-181a-1 (red arrow) and CD63-GFP-positive vesicle (green arrow) co-trafficked along the axon shaft to the growth cone (delineated with dashed white lines) wrist (white arrowhead) and central domain (white star).
Values are mean ± SEM (E, F). Statistics: **(E)** Total number of puncta counted: 174 (MB+), 224 (CD63+). **(F)** Data were normally distributed (Shapiro-Wilk test). Unpaired two-tailed t-test. Total number of puncta counted: 57 anterograde, 59 retrograde. (E,F) Data from 17 single axons from 5 independent experiments. Abbreviations: ns, not significant. Scale bars: 5 µm (B, C, D, G).

[S5] Figure S5: Validation of axonal sample preparation and translation- dependent cue-induced collapse, related to Figure 5
(A) Representative image of stage 37/38 RGC axons cultured for 24 hours, before and after explant removal. Zoom-in panels illustrate that growth cones still adopt a stereotypical shape after removing the explant ("cut") suggesting that axonal health is maintained; axons also stay responsive to cues as demonstrated by Sema3A-induced collapse. **(B)** RT-PCR from RNA extracted from isolated axons or from

stage 37/38 whole eyes. β-Actin mRNA is present both in eye and axons, while MAP2 mRNA is present only eye, suggesting absence of dendritic material in the axonal samples. **(C)** Frequency (in percentage) of collapsed growth cones from stage 37/38 embryos, following a 10 min (200 ng/mL) Sema3A bath application. 50 µM cycloheximide (CHX) was applied to block translation. Total number of counted growth cones is reported in the column. **(D)** Quantification of the expression levels of miRNAs using the $2^{(-\Delta Ct)}$ method and U6 as normalizer.
Values are mean ± SEM (C,D). Statistics: *** p<0.001, **** p<0.0001. **(C)** Two-way ANOVA followed by Tukey's multiple comparison post-hoc test, n=4 independent experiments. **(D)** Data were normally distributed (Shapiro-Wilk test). One-way ANOVA followed by Tukey's multiple comparison post-hoc test, n=3 independent experiments (RNA was collected from stage 40 isolated axons for each experiment). Abbreviations: Ax, isolated axon; ns, not significant; NT, no template RT negative control; CHX, cyclohexamide; -, no template PCR negative control. Scale bars: 50 µm (A, left), 30 µm (A, right).

[S6] Figure S6: Morpholino mix validation, related to Figure 6
(A, D) Schematic representation of the experimental paradigm. **(B,C)** Quantification of the expression levels of miRNAs using the $2^{(-\Delta Ct)}$ method and U6 as normalizer, from stage 40 eyes derived from either 150 µM MOs-5p or co-MO **(B)** or 200 µM MOs-3p or co-MO **(C)** microinjected embryos. Data are presented normalized to co-MO. **(E, F)** Quantification of the expression levels of miR-181a-1-3p (E) and miR-181a-5p (F) using the $2^{(-\Delta Ct)}$ method and U6 as normalizer, from axons transfected with 2 µM MOs-5p, MOs-3p or co-MO. Data are presented normalized to PBS control.
Values are mean ± SEM throughout the figure. Statistics: * p<0.05. **(B, C, E, F)** Data were not normally distributed (Shapiro-Wilk test). Two-tailed Mann Whitney test. (B, C, E) n=4; (F) n=3 independent experiments. Abbreviations: ns, non-significant.

[S7] Figure S7: Mimics rescue miR-181 loss of expression, related to Figure 7
(A) Schematic representation of the experimental paradigm. Microinjection mixture: pre-miR-181a-1-, pre-miR-181a-2- and miR-181b-MO at 0.4 ng each in 1 nL (miR-181-MO) and custom control plus standard control MOs (co-MO) at 0.6 ng each in 1 nL. Electroporation mixture concentration: 0.5 µg/µl pCS2 + mCherry plasmid; 50 µM miRNA mimic cocktail (25 µM miR-181a-mimic + 25 µM miR-181b-mimics or 50 µM control mimics). **(B)** ISH on cryosections using miR-181a and b specific LNA probes. miR-181a and b are distributed in the inner nuclear and ganglion cell layer. Note the absence of signal upon miR-181 loss-of-function and how this signal is rescued specifically in areas electroporated with miR-181a and b mimics. **(C)** ISH on cryosections as in (B) where brain and contralateral eye to the electroporated retina are also visible. Note the absence of miR-181 signal in both right and left retina except in the electroporated region (red arrow, delineated with dashed black lines). **(D)** Frequency distribution (in percentage) of the amount of time embryos spent on average on black background. "Blind" indicates eyeless embryos. Numbers on the columns are the total number of analyzed embryos.
Values are mean ± SEM. Statistics: **** p<0.0001. **(D)** Data were not normally distributed (Shapiro-Wilk test). Two-tailed Mann Whitney test, n=4 independent experiments. Abbreviations: co-MO, control morpholino; miR-181-MO, morpholino mix targeting the miR-181 family (miR-181a and miR-181b); RPE, retinal pigment epithelium; NR, neural retina. Scale bar: 50 µm (B, C).

[S8] Figure S8: FRAP construct and experimental paradigm, related to Figure 8
(A) Schematic of Venus-3'UTR constructs used as reporters of axonal translation in FRAP experiments. **(B)** Quantification (in percentage) of the axonal fluorescence recovery after photobleaching (FRAP) of Venus-ACTB-3'UTR construct *ex vivo* using whole explants. **(C)** Representative growth cones depicting Venus fluorescence intensity as a heatmap. **(D, E)** Schematic representations of the experimental paradigms. **(E)** Axons in the vicinity of tectal Sema3A expression territories were selected for FRAP analysis. **(F)** Proposed model: pre-miR-181a-1 is transported along RGC axons tethered to CD63-positive vesicles. Under non-stimulated conditions TUBB3 undergoes basal translation in the axonal compartment. Upon Sema3A exposure, pre-miR-181a-1 and pre-miR-181a-2 are locally processed and the expression level of the concomitant newly synthesized miRNAs increase locally within the growth cone. miR-181a-5p, the

predominant mature miRNA generated from pre-miR-181a-1 and pre-miR-181a-2, targets TUBB3, thereby silencing protein synthesis through LPS inhibition (LPS-I).
Values are mean ± SEM. Statistics: **** p-value<0.0001. **(B)** Dashed black lines represent least-squares fits to a single-exponential decay equation. Numbers of single axons analyzed are reported between brackets. n=3 independent experiments. Row statistics are reported in Table 4. Abbreviations: ACTB, β-Actin; bp, base pair; CHX, cyclohexamide; TUBB3, tubulin beta 3 class III; APP, Amyloid precursor protein; THBS1, Thrombospondin 1. Scale bar: 10 μm (C).